# Self-Assembly Micelles from Novel Tri-Armed Star C₃-(PS-*b*-PNIPAM) Block Copolymers for Anticancer Drug Release

**Feng Xu, Jing-Wen Xu, Bi-Xia Zhang, and Yan-Ling Luo**

Key Laboratory of Macromolecular Science of Shaanxi Province, School of Chemistry and Chemical Engineering, Shaanxi Normal University, Xi'an 710062, P. R. China

*Novel tri-armed star polystyrene-block-poly(N-isopropylacrylamide) block copolymers with trimesic acid as central molecules were synthesized by successive two-step atom transfer radical polymerization, and confirmed by Fourier-transform infrared spectra, ¹H nuclear magnetic resonance, and laser light scattering gel chromatography system. The copolymers could self-assemble into spherical core-shell micelles in aqueous media independent on drug loading. Physicochemical properties of the blank and drug-loaded micelles were examined by surface tension, fluorescence spectroscopy, UV-vis, transmission electron microscope, and dynamic light scattering measurements. The copolymer micelles exhibited thermo-triggered phase transition, with low critical solution temperature of 33.7 and 34.6°C, varying with copolymer compositions. The critical aggregate concentrations were 11.62 and 47.61 mg $L^{-1}$, and hydrodynamic diameters from 200 to 220 nm. Water-insoluble 10-hydroxycamptothecine was encapsulated into the micelle aggregates to investigate the change in the resulting physicochemical parameters, thermo-triggered in vitro drug release, and the applicability as drug targeting release carriers. MTT assays were carried out to uncover cytotoxicity of the newly developed micelle-based drug formulations. © 2014 American Institute of Chemical Engineers AIChE J, 61: 35–45, 2015*
*Keywords: biomaterials, drug release, polymer properties, self-assembly*

## Introduction

In the past few years, it is an interesting topic to study synthesis of star polymers with controlled compositions, architectures, and functionalities. Living radical polymerization processes, including stable free radical polymerization,[1,2] reversible addition-fragmentation chain transfer polymerization,[3,4] and atom transfer radical polymerization (ATRP),[5–9] have turn out to be versatile for the synthesis of the polymers with well-defined structures and complex architectures and have proved a considerable growth. There are two methods for preparing star polymers: the "arm-first" and the "core-first." The arm-first technique tends to prepare the arms primarily and subsequently coupled to the core. However, because of steric effects, complete functionalization of the core is often not achieved using this approach. However, the core-first method allows better control over the star polymer architecture.[5,10,11]
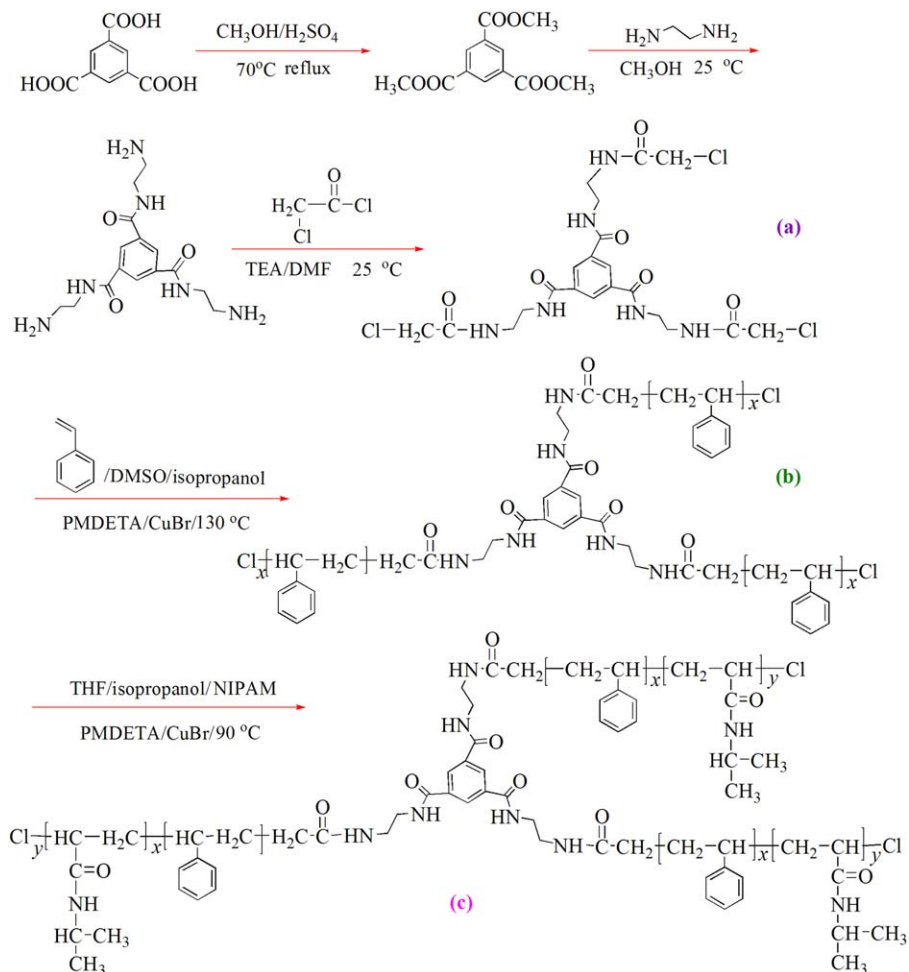
Star copolymers contain a distinct central branching point with several polymeric arms. This architecture of star copolymers has a pronounced impact on the solution self-assembly of the block copolymers, which leads to formation of nanostructured polymeric micelle aggregates, when compared to linear block copolymers with identical molecular weight.[5,12–14] The driving force for this aggregation is the reduction of surface area of the insoluble block in the nonsolvent.[15] So far, star polymer micelles derived from the amphiphilic block copolymers have attracted broad interest in the field of gene and drug targeted delivery owing to their great potential acting as carries for both imaging and therapy.[16–22] Compared to linear amphiphilic copolymer micelles, the star copolymer micelles are more stable because they contain covalently fixed branching points that can encapsulate a hydrophobic drug in aqueous media. Moreover, the micelle core is made up of the hydrophobic segments of the copolymer and serves as a reservoir to solubilize hydrophobic drugs, protects them against *in vitro* and *in vivo* degradation, and controls their release. The micelle shell, made up by the hydrophilic polymer segments, maintains the colloidal stability and aqueous solubility of the micelle. Polymeric micelles have shown excellent performances as drug delivery systems and several formulations are now undergoing clinical trials.

Poly(*N*-isopropylacrylamide) (PNIPAM) is the most widely investigated thermoresponsive polymer, which exhibits a reversible sharp phase transition in water at around 32°C.[23,24] A number of attentions have been focused on the copolymers consisting of NIPAM from the view of advanced materials for their extensive applications, such as a temperature dependent controlled release system and nanotechnology. In the context of the above description, we reported a novel tri-armed star-like polystyrene-*block*-PNIPAM block copolymer, C₃-(PS-*b*-PNIPAM), by esterification, aminolysis, and two successive ATRP processes. Chemical structure and

---

**Scheme 1. Schematic diagram of representative synthesis process of thermosensitive C₃-(PS-*b*-PNIPAM) copolymers.**

[Color figure can be viewed in the online issue, which is available at wileyonlinelibrary.com.]

molecular weight were well characterized, physicochemical properties of the copolymer micelles were sufficiently investigated, and drug loading capacity (lc) and *in vitro* drug release were evaluated. These amphiphilic star block copolymers are expected to have potential applications in the field of biotechnology as drug targeted release carriers.

## Experimental Section

### Materials and reagents

1,3,5-Benzenetricarboxylic acid or trimesic acid (95%) was obtained from the Sinopharm Chem. Reagent Co., China, and used without further purification. Chloroacetyl chloride (CC, 98.5%) was purchased from the Aladdin Reagent Company, and used as received. Styrene (98%) was supplied by the Sinopharm Chem. Reagent Co., China, and washed with 5% NaOH to remove polymerization inhibitor, followed by deionized water to scour till it was neutral, and then dried over anhydrous magnesium sulfate and distilled before use. *N*-isopropyl acrylamide (NIPAM, 98%) was bought from the Aladdin Reagent Company, and recrystallized from *n*-hexane and dried in vacuum for 24 h prior to use. Triethylamine (TEA or Et₃N) was obtained from the Sinopharm Chem. Reagent Co., China, and dried over CaH₂ and distilled before use. *N,N,N′,N′, N″*-pentamethyldiethylenetriamine (PMDETA, 98%) was purchased from the Alad-

din Reagent Company, and used without further purification. Both tetrahydrofuran (THF, analytical grade) and *N,N*-dimethylformamide (DMF, 99.5%) were provided by the Alfa Aesar and dried over CaH₂ and distilled before use. Methanol (99.5%) and ethylenediamine (EDA, 98%) were from the Xi'an Chemical Reagent Factory, and dried over KOH. 10-Hydroxycamptothecine (HCPT, 98%), an anticancer drug, was provided by the Capot Chemical Co., China.

### Synthesis methods

Tri-armed star polystyrene-*block*-poly(*N*-isopropylacrylamide) (abbreviated as C₃-(PS-*b*-PNIPAM)) block copolymers were synthesized via the following five-step reaction, as shown in Scheme 1.

### Synthesis of trimethyl benzene-1,3,5-tricarboxylate

Trimethyl benzene-1,3,5-tricarboxylate (TMBT) was prepared in accordance with the method reported elsewhere.[25–27] A 100-mL three round bottom flask fitted with a magnetic stirrer and a heating oil bath was charged with 3 g (0.014 mol) of 1,3,5-benzenetricarboxylic acid, 30 mL (0.742 mol) of methanol, and 1.5 mL oil of vitriol. The mixture was heated up to 70°C and refluxed for 6 h, and finally cooled to room temperature. A white power TMBT (Yield: 97%) was obtained after filtered, washed with methanol, and dried in vacuum at room temperature for 24 h. Fourier-

**Table 1. Formulations, Codes, and LLS-GCS Data of the Resulting Copolymers**

| Samples | Mole Ratios[a] | Mn | | $M_w$[b] | PDI[b] | Styrene/NIPAM in Each Arm (mol)[c] | Yield (%) |
| | | NMR | LLS-GCS | | | | |
| --- | --- | --- | --- | --- | --- | --- | --- |
| C₃-PS | 1:200 | 26,830 | 39,941 | 64807 | 1.62 | | 55.0 |
| C₃-(PS-b-PNIPAM)₁ | 1:300 | 30,570 | 43,544 | 72401 | 1.64 | 86/11 | 39.4 |
| C₃-(PS-b-PNIPAM)₂ | 1: 600 | 31,580 | 45,772 | 71261 | 1.58 | 86/14 | 41.0 |

[a]Molar ratios of C₃ to styrene or C₃-PS-(Cl) to NIPAM.
[b]As determined by LLS-GCS.
[c]As determined by NMR spectroscopy.

transform infrared spectra (FT-IR; $v$, cm$^{-1}$): 1740 (—C=O stretch), 2959–3100 (Ar—H stretch), 2846–2959 (—CH₃ stretch), 1447 (—CH₃ bending), 1495 and 1600 (aromatic skeleton stretch), 1252 (—C—O stretch), 740 and 878 (C—H out-of-plane bending of three substituted benzene rings). ¹H nuclear magnetic resonance (¹H NMR; 300 MHz, DMSO-$d_6$): $\delta$ (ppm) = 8.60 (s, 3H, Ar—H), and 3.93 (s, 9H, —COOCH₃).

### Synthesis of 1,3,5-benzene tricarboxylic acid tris-N-(2-aminoethyl) amide

1,3,5-Benzene tricarboxylic acid tris-N-(2-aminoethyl) amide (BTATAA) was attained by amination reaction of EDA reported elsewhere.[25,28–32] Flesh EDA of 20 mL (0.3 mol) was added into a 100-mL three flask, and then 0.63 g (2.5 mmol) TMBT dissolved in 40 mL methanol in advance was slowly added into the solution by a constant pressure funnel. The mixture was stirred under nitrogen atmosphere at 0°C for 30 min, and then at 25°C for 24 h. Excess EDA was removed by rotary evaporation, and then, the resultant crude product was dissolved in methanol/toluene (1/10 by volume) mixed solvents and re-evaporated to remove the residual EDA. The process was repeated three times and a sticky solid mass, BTATAA, was obtained (Yield: 90%). FT-IR ($v$, cm$^{-1}$): 3285–3355 (—NH₂ and —NH stretch), 2933–3075 (Ar—H stretch), 2870–2933 (—CH₂ stretch), 1659 (—C=O stretch), 1545 (—NH₂ and —NH bending), 1430 (—CH₂—bending), 1480 and 1600 (aromatic skeleton stretch), 1283 (—C—N), 720 and 825 (C—H out-of-plane bending of three substituted benzene rings). ¹H NMR (300 MHz, D₂O): $\delta$ (ppm) = 8.00 (s, 3H, Ar—H), 3.34 (m, 6H, —CONHCH₂—), 2.75 (m, 6H, —NHCH₂CH₂NH₂).

### Synthesis of a small molecular star initiator (C₃)

C₃ was achieved via an aminolysis reaction of BTATAA with CC according to literatures.[31,33] 0.798 g (4.74 mmol) BTATAA was dissolved in 20 mL dried DMF in a 100-mL three round bottom flask, and 1.19 mL (17.1 mmol) TEA was injected. After the solution temperature was tuned at 0°C in an ice-water bath, 0.64 mL (17.1 mmol) chloroacetyl chloride was slowly dropped into the reaction solution under nitrogen atmosphere within 3 h with stirring. The reaction mixture was further stirred at 25°C for 24 h. The resultant mixture was allowed to sit for 2 h and then filtered to remove quaternary ammonium salt. The filtrate was evaporated under reduced pressure to remove most of the solvent. The pure product (star initiator C₃) was obtained by column chromatography on silica gel using CH₃OH/CH₂Cl₂ (1:12 by volume) to separate unreacted raw materials and possible by-products (single- and disubstituted products). Yield: 56.2%. FT-IR ($v$, cm$^{-1}$): 3285 (—NH— stretch), 2756–3080 (Ar—H and —CH₂—), 1659 (—C=O stretch), 1545 (—NH—

bending), 1283 (—CN bending). ¹H NMR (300 MHz, DMSO-$d_6$): $\delta$ (ppm) = 8.89 (s, 3H, Ar—H), 8.55 (s, 6H, —CONHCH₂CH₂NHCO—), 4.09 (s, 6H, —NHCOCH₂Cl), 3.04–3.09 (m, 12H, —CONHCH₂CH₂NHCO—).

### Synthesis of star-like polystyrene (C₃-PS or C₃-PS-(Cl))

C₃-PS-(Cl) was prepared by ATRP, with PMDETA as ligand, CuCl as catalyst, and C₃ as initiator. Typically, 0.25 g (0.5 mmol) C₃, 11.50 mL (100 mmol) styrene, 0.17 mL (1 mmol) PMDETA, and 6 mL DMSO/isopropanol (3 mL/3 mL) mixture solvent were added into a Schlenk flask. After the mixture was deoxygenated by a repeated freeze-pump-thaw process for two times, 0.0495 g (0.5 mmol) CuCl was added to the mixture. The mixture was again deoxygenated by the above same operation and then the reaction was performed at 130°C for 24 h with stirring. The resultant mixture was passed through an activated neutral Al₂O₃ column to remove copper complex. After the mixture solution was concentrated by rotary evaporation to remove most of solvent, it was put into a dialysis bag with molecular weight cut off 10,000 to remove unreacted monomer and residues of initiator and solvent. The dialysate was dried by lyophilization and a white solid product was obtained (Yield: 55%). FT-IR ($v$, cm$^{-1}$): 3325–3387 (—NH— stretch), 2826–3012 (Ar—H, —CH, and —CH₂ stretch), 1656 (—C=O stretch), 1533 (—NH— bending), 1430 (—C—H bending), 1062–1200 (—C—N stretch), 660–725 (C—H out-of-plane bending of both single (main) and three substituted benzene rings). ¹H NMR (300 MHz, CDCl₃): $\delta$ (ppm) = 7.70–8.09 (s, signals a, d, and e′, Ar—H in center molecules and —NH—), 6.58–7.09 (m, signals i, j, and k, Ar—H in PS), 3.75 (m, signals b′ and c, 12H, —CONHCH₂CH₂NHCO—), 1.86 (m, signal h, —CH₂CHC₆H₅—), 1.43–1.53 (m, signal g, —CH₂CHC₆H₅—).

### Synthesis of C₃-(PS-b-PNIPAM) block copolymers

C₃-(PS-b-PNIPAM) was synthesized by a successive ATRP at molar ratios of C₃-PS-(Cl) to NIPAM 1:300 and 1:600 (Table 1). PMDETA (Approximately 2 with respect to the molar or equivalent ratio of initiator), THF/isopropanol (3 mL/3 mL) mixed solvents were added to the Schlenk flask. The mixture was deoxygenated by a repeated freeze-pump-thaw process for two times, and then CuCl (Approximately 1 with respect to the molar or equivalent ratio of initiator) was added to the mixture. The mixtures were deoxygenated by the freeze-pump-thaw process once again. The reaction was carried out at 90°C for 24 h to complete the polymerization. The resultant mixture was passed through an activated neutral Al₂O₃ column to remove copper complex, and then, the solution was concentrated by rotary evaporation to remove most of solvent. The concentrated solution was put into a dialysis bag (MWCO: 40,000) to

remove unreacted monomer and residues of initiator and solvent. The dialysate was dried by lyophilization and a white solid mass was obtained (Yield: 41%). FT-IR spectra ($v$, cm$^{-1}$): 3296 (—NH— stretch), 2850–3072 (Ar—H, —CH—, —CH$_2$—, and —CH$_3$ stretch), 1656 (—C═O stretch), 1543 (—NH— bending), 1450 (—C—H bending), 1062–1170 (—C—N stretch), 696–757 (C—H out-of-plane bending of both single (main) and three substituted benzene rings). $^1$H NMR (300 MHz, CDCl$_3$): $\delta$ (ppm)= 7.70–8.09 (s, signals $a$, $d$, and $e'$, Ar—H and —NH—), 6.58–7.04 ($m$, signals $i$, $j$, and $k$, Ar—H), 6.58 ($d$, signal $n$, —CONHCH(CH$_3$)$_2$), 3.86–4.00 ($m$, signal $m$, —NHCH(CH$_3$)$_2$), 3.70 ($m$, signals $b'$ and $c$, 12H, —CONHCH$_2$CH$_2$NHCO—), 1.14 ($d$, signal $l$, —NHCH(CH$_3$)$_2$), 1.86 ($m$, signals $h$ and $p$, —CH$_2$CHC$_6$H$_5$— and —CH(CONHCH(CH$_3$)$_2$)CH$_2$—), 1.42 ($m$, signals $g$ and $o$, —CH$_2$CHC$_6$H$_5$— and —CH(CONHCH(CH$_3$)$_2$)CH$_2$—).

### Structural characterization

FT-IR of the block copolymers were recorded on an AVATAR 360 ESP FT-IR spectrometer (Nicolet), and samples were pressed in KBr pellets. $^1$H NMR spectra were obtained on an Avance 300 MHz NMR spectrometer (Bruker, Germany) with tetramethylsilane as internal standard. The absolute molecular weight of the star block copolymers was determined by laser light scattering gel chromatography system (LLS-GCS, VISCOTEK TM, Malvern Instruments, England), equipped with a pump module (GPCmax, Viscotek Corp., Houston, TX), a combined light-scattering detector (Model 270 Dual Detector, Viscotek Corp.), and a refractive index detector (VE 3580, Viscotek Corp.). Two columns 7.8 × 300 mm (LT5000L, Mixed, Medium Org and T6000M, Mixed, General Org) were used for the THF eluent at 35°C (flow rate: 1 mL min$^{-1}$). Data were analyzed using Viscotek OmniSEC software. Before measurement, the samples solutions dissolved in THF were filtered through a 0.45 $\mu$m (pore size) needle-type filter (organic, diameter: Φ13 mm).

### Physicochemical characterization

The micellization behavior analyses were performed by a surface tension technique. (HCPT-Loaded) Copolymer micelle solutions of 40 mL with different concentrations (the concentration range from 5 × 10$^{-5}$ to 5 × 10$^{-1}$ mg mL$^{-1}$) were prepared and equilibrated at room temperature overnight, and the surface tension was recorded on a DCAT 21 tensiometer (Data Physics, Germany) using the Wilhelmy plate method. The critical aggregate concentration (CAC) was estimated from plots of the static surface tension vs. the logarithm of the concentration.

The CAC values were also determined on a Perkin Elmer LS55 fluorescence spectrophotometer (PE) using pyrene as a probe. Micelle solutions with a concentration range from 5 × 10$^{-1}$ to 5 × 10$^{-5}$ mg mL$^{-1}$ were prepared while the concentration of pyrene in the copolymer solution in each flask was adjusted to 6.0 × 10$^{-7}$ mol L$^{-1}$. The emission wavelength was 394 nm. The slit width for both excitation and emission was 10 nm. The wavelength range for measurements is from 290 to 360 nm with an emission wavelength of 394 nm. The CAC values were achieved by the $I_{337}/I_{333}$ ratios vs. logarithm of polymer concentrations.

The morphologies of (HCPT-loaded) copolymer micelles were analyzed by a JEM-1210 transmission electron microscope (TEM, JEOL, Japan) at an acceleration voltage of 200 kV. Before measurement, a drop of freshly-prepared micelle solutions containing 2 wt % phosphotungstic acid was

dipped on a copper grid with carbon films and dried at room temperature.

The micellar size and size distribution analyses were performed using a dynamic light scattering (DLS, BI-90Plus) equipped with an argon ion laser operating at $\lambda = 660$ nm, a deflection angle of 90° and output power of 15 mW at room temperature. 40 mL block polymer micelle solutions with concentration of 500 mg L$^{-1}$ were taken for measurement, and each sample was repeated in triplicate.

Thermosensitivity of (HCPT-loaded) block copolymer micelles was examined based on the turbidity and size change, which was measured at various temperatures by monitoring the turbidity or optical transmittance and hydrodynamic diameters ($D_h$). The cloud points or low critical solution temperature (LCST) of the polymer solution (Concentration: 100 mg L$^{-1}$) was defined as the temperature producing a half decrease of the total decrease in transmittance, and measured on a U-3900/3900H UV-vis spectrophotometer (Hitachi, Japan) at 500 nm.

### Preparation of drug-loaded micelles

Drug-loaded micelle was prepared using the membrane dialysis method. Briefly, about 20 mg C$_3$-(PS-$b$-PNIPAM) and 4 mg HCPT were dissolved in 6 mL DMF, and then, the solution was vigorously stirred at room temperature for 2 h. Subsequently, the deionic water was added into the mixture solution until the solution became opalescent. The mixture solution was transferred into a dialysis bag (MWCO: 5000 Da) to dialyze against deionic water for 12 h to remove DMF, and the water was renewed once every 3 h. The dialysate was dried by lyophilization and the drug-loaded micelles were collected. To determine the drug loading capacity (LC) and entrapment efficiency (EE), the lyophilized drug-loaded micelles were dissolved in DMF and analyzed by UV absorbance at 391 nm, using a standard calibration curve experimentally obtained with HCPT/DMF solutions. The LC and EE were calculated according to the following formulas

$$LC(wt\%) = (\text{Mass of drug in micelles/Mass of block polymer in formulation}) \times 100 \quad (1)$$

$$EE(wt\%) = (\text{Mass of drug in micelles/Mass of the feeding drugs}) \times 100 \quad (2)$$

### In vitro drug release measurements

The *in vitro* release experiments were carried out at simulated physiological media of pH 7.4 and different temperatures. Typically, 4 mg lyophilized HCPT-loaded copolymer micelles were dispersed in 4 mL PBS solutions of pH 7.4 and were placed into dialysis bag (MWCO: 8000), and then immersed into 400 mL PBS solutions of pH 7.4 and kept in a shaking water bath at 25 and 37°C. PBS solutions of 4 mL were taken out from the solution periodically, and the volume of solution was kept constant by adding 4 mL fresh PBS after each sampling. The concentration of the drug in the release samples was determined by UV absorbance at 391 nm. The cumulative drug release (wt %) was calculated on the basis of the following formula

$$\text{Cumulative drug release } \% = M_t/M_0 \times 100 \quad (3)$$

where $M_t$ is the amount of drug release at $t$ time, and $M_0$ stands for the amount of drug loaded in the copolymer micelles.

### MTT assay

The cytotoxicity of the blank, HCPT-loaded micelle aggregates was assessed by MTT assay with L929 mouse embryonic fibroblasts. Cells were seeded into a 96-well plate at a density of $1 \times 10^4$ cells well$^{-1}$, cultured overnight and then incubated with the blank and HCPT-loaded micelles in a complete Dulbecco's modified eagle's medium containing 10% hyclone fetal bovine serum (high glucose DMEM) at 37°C in 5% $CO_2$ atmosphere for 24 h before assay. To determine the cytotoxicity, blank, HCPT-loaded micelle solutions with various concentrations in complete DMEM were used to replace the culture medium and the cells were further cultured for 48 h. After that, the medium was replaced by 100 $\mu$L of fresh DMEM, followed by adding 20 $\mu$L of MTT stock solution (5 mg mL$^{-1}$) to the fibroblasts. After incubation for an additional 4 h, the supernatant was discarded, and then 150 $\mu$L of DMSO was added and shaken for 10 min at room temperature. At the same time, cells were seeded in a fresh culture medium (negative control) under the same conditions for reference. The optical density (OD) was monitored at 490 nm by a 96-wells universal microplate reader (Model 680, Bio-Rad laboratories, UK), and the cell viability was calculated as follows

$$\text{Cell relative viability} \% = (\text{OD}_{samples}/\text{OD}_{control}) \times 100\% \quad (4)$$

where $\text{OD}_{control}$ and $\text{OD}_{sample}$ were obtained in absence of and in presence of blank and HCPT-loaded micelles, respectively. The Student;s $t$-test was used to determine the significance of any pairs of observed differences. Differences were considered statistically significant when $P < 0.05$. All quantitative results are reported as mean values $\pm$ standard deviation from data obtained from at least three separate experiments.

## Results and Discussion

### Synthesis and characterization of $C_3$-(PS-b-PNIPAM) block copolymers

Synthesis of tri-armed star $C_3$-(PS-b-PNIPAM) block copolymers based on trimesic acid as central molecules involves five-step successive processes, as demonstrated in Scheme 1. To attain an initiator with unique structure for ATRP, TMBT was prepared by the esterification reaction between methanol and trimesic acid, and then BTATAA was synthesized by amination reaction of EDA. Hence, a small molecular star initiator (structure (a) in Scheme 1), named $C_3$, was achieved via an aminolysis reaction of BTATAA with chloroacetyl chloride in DMF at room temperature.

FT-IR and $^1$H NMR are used to identify the chemical structure of these precursors (See Figures S1(A) and 2(A) in Supporting Information). The appearance of characteristic absorption peaks at 1740, 2921–3100, 2846–2921, 1447, 1495–1600, 1252, 740, and 878 cm$^{-1}$ preliminarily discloses the synthesis of TMBT (Supporting Information Figure S1(A)-a), and the hydrogen proton shift signals at 3.93 and 8.60 ppm further support the successful synthesis of TMBT (Supporting Information Figure S2(A)-a). Compared to TMBT, BTATAA produces new vibration bands at 3284–

3352, 1659, 1545, and 1283 cm$^{-1}$, which belongs to primary/secondary amine (—NH$_2$/—NH—) stretch, amidocarbonyl stretch, —NH$_2$/—NH— bending and —C—N stretch modes, respectively (Supporting Information Figure S1(A)-b). In the case of D$_2$O as solvent, three characteristic hydrogen chemical shift signals emerge at 8.00, 3.34, and 2.75 ppm, which are ascribed to the hydrogen proton of benzene rings (Ar—H), methylene protons next to acylamino groups (—CONHCH$_2$—) and methylene protons next to amido groups (—CH$_2$CH$_2$NH$_2$), respectively (Supporting Information Figure S2(A)-b), confirming the synthesis of BTA-TAA.[28] In the case of the star initiator (Supporting Information Figure S1(A)-c), it can be seen that only the secondary amine (—NH—) stretch vibration at 3285 cm$^{-1}$ appears, whereas $^1$H NMR spectra (Supporting Information Figure S2(A)-c) shows distinct resonance signals at 4.09 ppm assigned to methylene protons in —NHCOCH$_2$Cl (signal $f$) and at 8.55 ppm ascribed to imino protons in —CONHCH$_2$CH$_2$NHCO— (signals $d$ and $e'$).

$C_3$-PS and $C_3$-(PS-b-PNIPAM) starlike block copolymers were synthesized by a successive ATRP process, as shown in Scheme 1. They were confirmed by FT-IR and $^1$H NMR (See Figure S1(B) and Figure S2(B) in Supporting Information). The $C_3$-PS polymer (Supporting Information Figure S1(B)-d) gives characteristic amidocarbonyl stretch at about 1656 cm$^{-1}$, —NH— stretch at 3325–3387 cm$^{-1}$, and Ar—H and —C—H stretch vibration bands at 2860–3012 cm$^{-1}$, especially C—H out-of-plane bending of single (main) substituted benzene rings at 660–725 cm$^{-1}$. In comparison with the initiator $C_3$, new chemical shift signals emerge at 1.43–1.53, 1.86, and 6.58–7.09 ppm, representing the proton signals of methylene (—CH$_2$CHC$_6$H$_5$—), methyne (—CH$_2$CHC$_6$H$_5$—) and primary Ar—H in PS repeating units in Supporting Information Figure S2(B)-d. The $C_3$-(PS-b-PNIPAM) copolymer has almost the same FTIR characteristics as the $C_3$-PS copolymer due to similar chemical groups (Detailed designations are described in the experimental section), but difference in relative intensities (Supporting Information Figure S1(B)-e). $^1$H NMR spectra, however, provide characteristic distinguishable shift signals attributed to PNI-PAM blocks, at 6.58 ppm partially ascribed to —CONHCH(CH$_3$)$_2$, at 1.86 ppm assigned to —CH$_2$CHC$_6$H$_5$— and —CH(CONHCH(CH$_3$)$_2$)CH$_2$—, and at 1.42 ppm belonging to —CH$_2$CHC$_6$H$_5$— and —CH(CONHCH(CH$_3$)$_2$)CH$_2$—. In particular, the methyne protons (—NHCH(CH$_3$)$_2$) at 3.86–4.00 ppm and methyl protons (—NHCH(CH$_3$)$_2$) at 1.14 ppm consumingly support the incorporation of PNIPAM blocks (Supporting Information Figure S2B (e)). All these corroborate the synthesis of starlike $C_3$-(PS-b-PNIPAM) block copolymers.

As the synthesized three-armed star copolymers are branched macromolecules, and gel permeation chromatography (GPC) measurements do not give the true molecular weight of the copolymers, light scattering or osmometry technique should be adopted. LLS-GCS bears the advantages of both GPC and light scattering measurements, without standard samples, and can determine the absolute weight-average molecular weight ($M_w$), the number-average molecular weight ($M_n$) and molecular weight distribution ($M_w/M_n$, or polydispersity index [PDI]). Therefore, LLS-GCS was used to measure the molecular weight, and the results are shown in Table 1. It can be seen that the molecular weight of the star block copolymers increases with increasing the [NIPAM]/[$C_3$-PS-(Cl)] molar ratios. The molecular weight
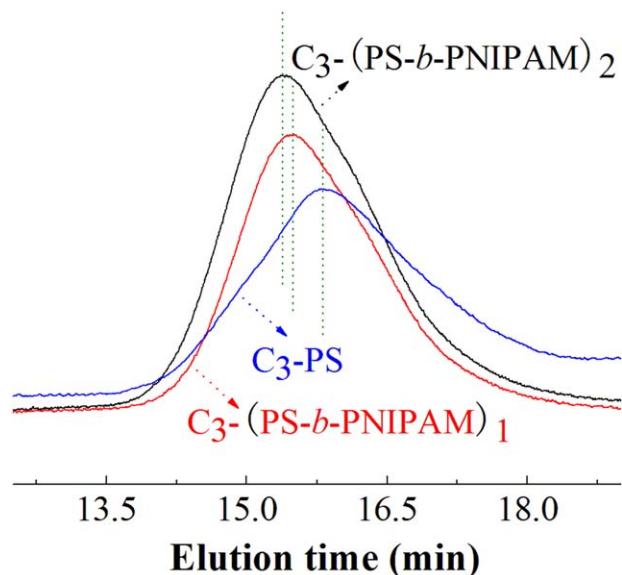
**Figure 1.** Plots of molecular weight distribution of C$_3$-PS precursor and C$_3$-(PS-*b*-PNIPAM) block copolymers.

[Color figure can be viewed in the online issue, which is available at wileyonlinelibrary.com.]

distribution is found to be a bit wide, with PDI about 1.58–1.64. However, plots of molecular weight distribution indicate that the star C$_3$-PS, C$_3$-(PS-*b*-PNIPAM)$_1$ and C$_3$-(PS-*b*-PNIPAM)$_2$ block copolymers produce monomodal and symmetrical elution peak, and there is no shoulder peak, no tailing in both lower and higher molecular weight regions whether they are intermediate or resultant products, as demonstrated in Figure 1. Therefore, there is no residual PS-Cl and monomer left after the ATRP polymerization reaction and dialysis. The elution peak of the C$_3$-(PS-*b*-PNIPAM) block copolymer emerges earlier than that of the C$_3$-PS, which can be regarded as an evidence of the formation of the star block copolymers. Hence, the polymerization process is well controlled and the product is effectively puri-

fied. In comparison with $M_w$ by GPC (Table S1 in Supporting information), the $M_w$ by LLS-GCS is higher, which may partially be due to the conformation differences between the GPC standard and the C$_3$-(PS-*b*-PNIPAM) molecules, and the existence of large C$_3$-(PS-*b*-PNIPAM) aggregates in LLS-GCS measurements. By the combination of FT-IR, $^1$H NMR, LLS-GCS results, it is concluded that the C$_3$-(PS-*b*-PNIPAM) block copolymer has successfully been synthesized.

Furthermore, the number of monomers per arm or the true composition of the copolymers was calculated by estimating the integration area ratios of the related shift peaks. Taking into the possible overlapping of chemical shift signals account, we have selected the Ar—H shift peak in the center molecule at ca. 7.96–8.09 ppm and the shift peak at 6.58–7.09 ppm related to Ar—H shift signals in the PS units or the —CH$_2$CHC$_6$H$_5$ peaks at 1.86–1.43 ppm for calculation so as to more accurately estimate the true composition. The experimental molecular weight of C$_3$-PS is about 26,830 (Table 1), and thus approximately 86 styrene monomeric units are incorporated in each initiating site of starlike initiators C$_3$, that is, the number of styrene monomer units per arm is 86. In the same way, the molecular weights of C$_3$-(PS-*b*-PNIPAM) star-like block copolymers are determined to be 30,570 and 31,580 by estimating the integration area ratio of the Ar—H peak in the PS units at 6.58–7.09 ppm to the —CH(CH$_3$)$_2$ peak in the NIPAM units at 3.86–4.00 ppm or to the —NHCH(CH$_3$)$_2$ peak at 1.14 ppm. The experimental molecular weights are higher than the GPC results (See also Table S1 in Supporting Information), but smaller than absolute molecular weights determined by LLS-GCS. It can be deduced from NMR measurements that about 33 and 42 NIPAM repeating units are connected with PS blocks or about 11 and 14 NIPAM repeating units are located at each PS branched block. The number of NIPAM monomer units per arm is about 11 and 14, and the block copolymers are named C$_3$-(PS-*b*-PNIPAM)$_1$ and C$_3$-(PS-*b*-PNIPAM)$_2$, respectively. The mole ratio of styrene: NIPAM units in the copolymer composition is about 8:1 and 6:1 in the case of C$_3$-(PS-*b*-PNIPAM)$_1$ and C$_3$-(PS-*b*-PNIPAM)$_2$, respectively.
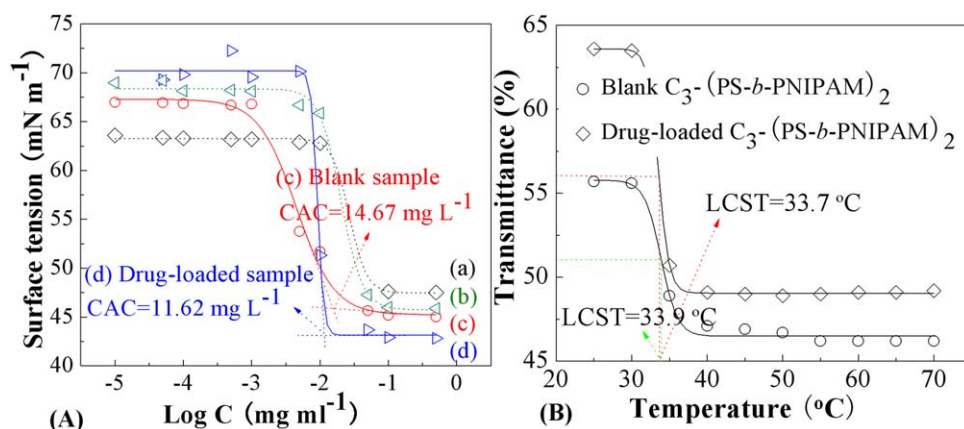


**Figure 2.** (A) Representative plots of static surface tension vs. the logarithm of C$_3$-(PS-*b*-PNIPAM) copolymer concentrations in aqueous solution: (a) blank and (b) drug-loaded C$_3$-(PS-*b*-PNIPAM)$_1$, and (c) blank and (d) drug-loaded C$_3$-(PS-*b*-PNIPAM)$_2$; and (B) transmittance dependence of blank and drug-loaded C$_3$-(PS-*b*-PNIPAM)$_2$ copolymer micelles on temperature at 500 nm (The polymer micelle concentrations: 100 mg L$^{-1}$).

[Color figure can be viewed in the online issue, which is available at wileyonlinelibrary.com.]

**Table 2. Physicochemical Parameter Changes of Blank and HCPT-loaded C₃-(PS-*b*-PNIPAM) Copolymer Micelles**

| Copolymer Micelles | $C_3$-(PS-*b*-PNIPAM)$_1$ | | $C_3$-(PS-*b*-PNIPAM)$_2$ | |
| --- | --- | --- | --- | --- |
| | Blank | HCPT-Loaded | Blank | HCPT-Loaded |
| CAC (mg L$^{-1}$) | 47.61 | 42.73 | 14.67 | 11.62 |
| LCST (°C) | 34.6 | 34.2 | 33.9 | 33.7 |
| $D_h \pm$ sd (nm) | 203.19 ± 7.20 | 210.17 ± 9.87 | 211.70 ± 4.97 | 217.77 ± 6.47 |
| PDI ± sd | 0.104 ± 0.019 | 0.246 ± 0.160 | 0.047 ± 0.052 | 0.076 ± 0.016 |

### Formation of the copolymer micelles and thermoresponsiveness

It is well known that polymer amphiphiles consisting of hydrophilic and hydrophobic segments can self-assemble and form micelle aggregates in an aqueous phase. To confirm the formation of micelles self-assembled from C₃-(PS-*b*-PNIPAM) copolymers, the surface tension alteration of the block copolymers in aqueous solution was measured. From the plot of static surface tension vs. the logarithm of the copolymer concentration, the CAC values of C₃-(PS-*b*-PNIPAM) copolymers in aqueous media are estimated, as shown in Figure 2A. It is clearly seen that the surface tension is relatively large at low concentrations. With increasing the concentrations of the copolymer solution, the surface tension decreases abruptly, indicating formation of micelles, and thus CAC is attained from the point of intersection in Figure 2A. The estimated CAC are about 14.67 and 47.61 mg L$^{-1}$ for C₃-(PS-*b*-PNIPAM)$_2$ and C₃-(PS-*b*-PNIPAM)$_1$, respectively (Table 2). The low CAC values suggest that the copolymer micelle aggregates are stable, and thus, the entrapped HCPT would not prematurely leak from the micelle aggregates during the circulation. Conversely, the low CAC value of C₃-(PS-*b*-PNIPAM)$_2$ than that of C₃-(PS-*b*-PNIPAM)$_1$ may be attributed to a reasonable hydrophilic/hydrophobic balance for the copolymer with longer NIPAM chains, which is more conducive to the formation of the polymer micelle aggregates.

Fluorescence spectroscopy was also used to determine the CAC of the copolymer micelles and to compare with values from surface tension experiments. Figures 3A depicts a representative excitation spectrum of pyrene probe of the C₃-(PS-*b*-PNIPAM)$_2$ copolymer with various concentrations in aqueous solution. It is clear that the fluorescence intensities increase from 332 to 336 nm with increasing the copolymer concentrations, signifying that the pyrene molecules are loaded into the copolymer micellar cores. The $I_{336}/I_{332}$ peak intensity ratios as a function of the logarithm of the copolymer concentrations can be used to express this change, and thus to determine the CAC values of the copolymer micelles from the plots. As shown in Figure 3B, and the C₃-(PS-*b*-PNIPAM)$_2$ copolymer micelle bears a CAC of 12.21 mg L$^{-1}$. Similarly, the CAC value of the C₃-(PS-*b*-PNIPAM)$_1$ copolymer micelle is determined to be 41.98 mg L$^{-1}$. These data are almost in agreement with those determined by the surface tension, and further indicate that long NIPAM chains more easily form the micelle aggregates.

Considering a thermoreversible phase transition behavior of PNIPAM homopolymers in aqueous solution, the LCST of the newly developed C₃-(PS-*b*-PNIPAM) tri-armed star block copolymer micelle aggregates was determined by a UV-vis spectrometer. Figure 2B shows transmittance change of representative C₃-(PS-*b*-PNIPAM)$_2$ sample with temperature in aqueous solution. It is seen from Figure 2B that an obvious phase transition emerges with temperature, and the LCST of the C₃-(PS-*b*-PNIPAM)$_2$ micelle is measured to be about 33.9°C. In the case of the C₃-(PS-*b*-PNIPAM)$_1$ sample, this value is about 34.6°C, as listed in Table 2. Clearly, the C₃-(PS-*b*-PNIPAM)$_2$ copolymer micelle with high
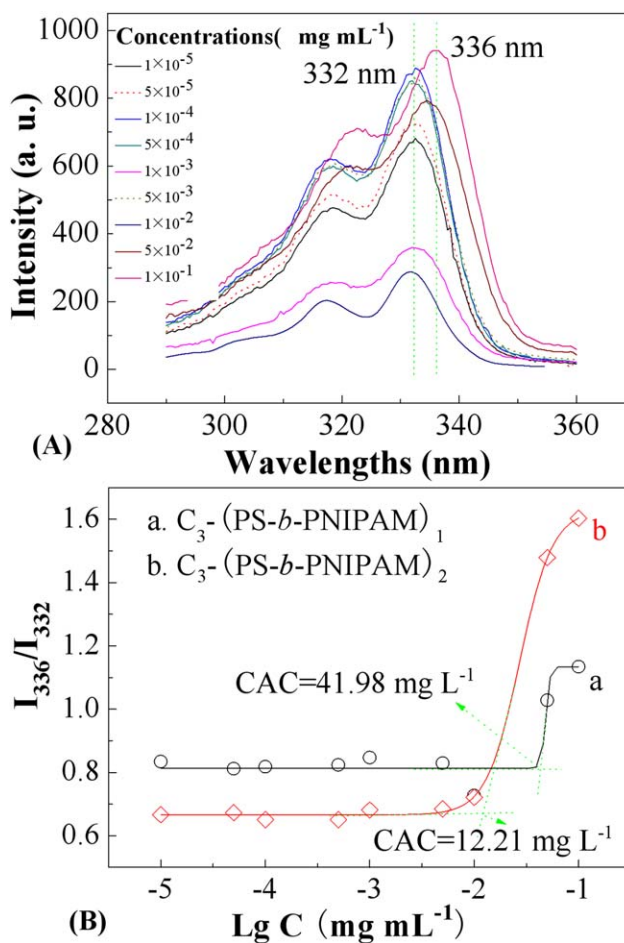
**Figure 3.** (A) Fluorescence excitation spectra recorded for pyrene equilibrated with C₃-(PS-*b*-PNIPAM)$_2$ copolymer micelles with various concentrations in deionized water, and (B) plots of the fluorescence intensity ratios $I_{336}/I_{332}$ from the excitation spectra of pyrene probe as a function of polymer concentrations (a: C₃-(PS-*b*-PNIPAM)$_1$ and b: C₃-(PS-*b*-PNIPAM)$_2$)).

[Color figure can be viewed in the online issue, which is available at wileyonlinelibrary.com.]
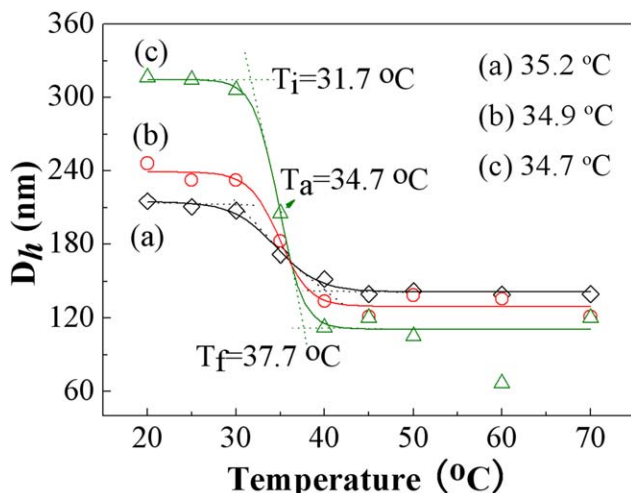
**Figure 4.** The changes in $D_h$ as a function of temperature for (a) blank $C_3$-(PS-*b*-PNIPAM)$_1$, (b) blank $C_3$-(PS-*b*-PNIPAM)$_2$ and (c) HCPT-loaded $C_3$-(PS-*b*-PNIPAM)$_2$ (The polymer micelle concentrations: 100 mg L$^{-1}$).

[Color figure can be viewed in the online issue, which is available at wileyonlinelibrary.com.]

molecular weight produces decreased LCST than the low molecular weight $C_3$-(PS-*b*-PNIPAM)$_1$ copolymer micelle. This LCST difference resulting from the molecular weight effect of PNIPAM blocks in the presence of identical length of PS blocks can be explained by the polymer–solvent interaction parameter ($\chi_c$) in Flory–Huggins theory[34]

$$\chi_c = 1/2(1 + r^{1/2})^2 \qquad (5)$$

As the molar volume ratios of polymer to solvent ($r$) decreases as the molecular weight decreases, $\chi_c$ increases, leading to increase in LCST of the $C_3$-(PS-*b*-PNIPAM)$_1$ copolymer micelle. Laukkanen, Furyk, and Xia et al.[34–36] once reported that the LCST of the polymers is inversely dependent on the molecular weight. The changes in size as a function of temperature for both the copolymer micelles are further investigated, as shown in Figure 4. It can be seen that the $D_h$ values of both the blank micelle aggregates are decreased with increasing the medium temperature due to the shrinkage or/and collapse of PNIPAM shells. In Figure 4, the point of intersection where the $D_h$ starts to decline is defined as $T_i$, and the point of intersection, at which the micelle size tends to be stable, is named $T_f$. In the narrow temperature range from $T_i$ to $T_f$, the micelle sizes changes

sharply with temperature. The average temperature of both $T_i$ and $T_f$ is defined as LCST values. It is thus inferred that the LCST values were approximately 35.2 and 34.9°C for blank $C_3$-(PS-*b*-PNIPAM)$_1$ and $C_3$-(PS-*b*-PNIPAM)$_2$, respectively. The HCPT-loaded $C_3$-(PS-*b*-PNIPAM)$_2$ copolymer micelle has LCST of 34.7°C. These results are almost in accordance with those by UV-vis transmittance analysis within the experimental errors, further corroborating thermo-triggered responsive properties.

In general, drug loading may influence the micelle stability[37,38] and thus cause physicochemical properties to be altered. To testify the applicability of the prepared three-armed star block copolymer micelle aggregates as hydrophobic drug carriers, the effect of the HCPT encapsulation on self-assembly micellization behavior of the block copolymers in aqueous solution is investigated, as illustrated in Figure 2 and Table 2. It is clearly noticed that the block copolymer micelle aggregates do not produce significant changes in the physicochemical properties after the HCPT is entrapped into the hydrophobic core, signifying that the drug loading would not do harm to the formation of the copolymer micelles. In comparison with the blank copolymer micelle aggregates, the CAC and LCST values of the HCPT-loaded copolymer micelles are more or less decreased. Especially, the decreased CAC values further verify the HCPT-loaded micelles are more stable than the blank counterparts. Consequently, the prepared copolymer micelles can safely load hydrophobic drug and be used for drug release applications by mediating their physicochemical properties themselves.

Polymer micelles as ideal drug targeting release carriers should bear small particle size, prolonged circulation, and accumulation in desired pathological sites in the body.[39] Small size of polymeric micelles is very important for providing passive tumor targeting ability via the enhanced permeability and retention effect. Meanwhile, morphologies, size, and size distribution of polymeric micelles affect the uptake characteristics of drugs encapsulated in the polymer micelles. Therefore, these physical parameters and topologies of blank and HCPT-loaded copolymer micelles are investigated by TEM and DLS. TEM photographs of representative $C_3$-(PS-*b*-PNIPAM)$_2$ copolymer micelles are displayed in Figure 5. It is clear that the blank and HCPT-loaded copolymers spontaneously assemble into core-shell spherical nanoscale micelles in aqueous solution at room temperature, with hydrophobic PS segments as an inner core and hydrophilic PNIPAM fragments as an external shell. It is also noticed from Figure 3 that as small molecular drug HCPT is entrapped into the PS hydrophobic cores, the HCPT-loaded $C_3$-(PS-*b*-PNIPAM)$_2$ copolymer micelle (Figure 5b)
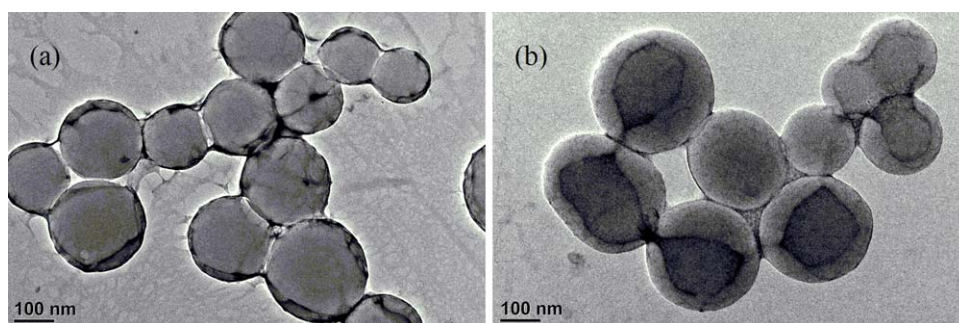


**Figure 5.** Representative TEM photographs of (a) blank and (b) drug-loaded $C_3$-(PS-*b*-PNIPAM)$_2$ copolymer micelles (The copolymer micelle concentration: 250 mg L$^{-1}$).
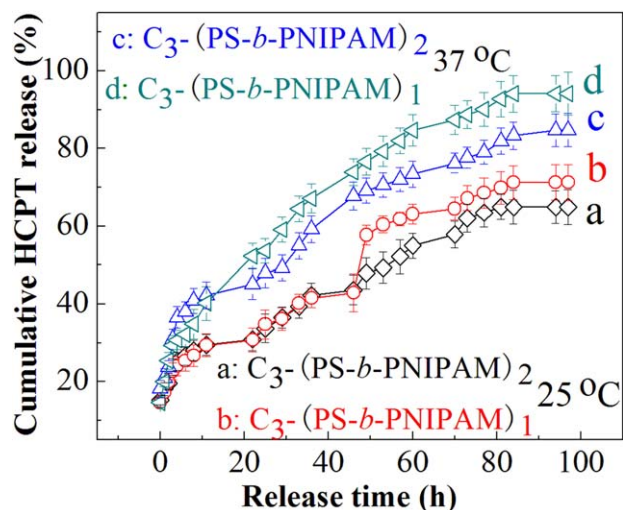
**Figure 6. Drug release profiles from (a and c) HCPT-loaded $C_3$-(PS-*b*-PNIPAM)$_2$ and (b and d) HCPT-loaded $C_3$-(PS-*b*-PNIPAM)$_1$ copolymer micelles in PBS solution of pH 7.4 at 25 and 37°C.**

[Color figure can be viewed in the online issue, which is available at wileyonlinelibrary.com.]

possesses a larger size than the blank $C_3$-(PS-*b*-PNIPAM)$_2$ copolymer micelle (Figure 5a), and the average TEM diameters are about 234 and 198 nm, respectively. The TEM size ranges are from 147 to 253 nm for the blank micelle, and from 200 to 307 nm for the HCPT-loaded counterpart. The DLS determination gives almost the consistent micelle sizes with TEM results, as tabulated in Table 2. The blank copolymer micelles have mean hydrodynamic diameters ($D_h$) in a range from about 203 to 212 nm, and the $D_h$ of the HCPT-loaded copolymer micelles changes from ca 210 to 218 nm, corresponding to $C_3$-(PS-*b*-PNIPAM)$_1$ and $C_3$-(PS-*b*-PNIPAM)$_2$, respectively. These results fully signify that HCPT is indeed entrapped into the core of the copolymer micelles. The increased $D_h$ values with increasing the molar ratios of hydrophilic NIPAM blocks may be ascribed to high molecular weight or chain length of hydrophilic NIPAM blocks. This is applicative to both the blank and HCPT-loaded copolymer micelles. These copolymer micelle nanoparticles have narrow particle-size distribution, with the PDIs less than 0.25. The small size and narrow size distribution endow the $C_3$-(PS-*b*-PNIPAM) copolymer micelles with good physicochemical performances as water-insoluble drug targeting release carriers.

### Drug loading and release studies

A suitable drug delivery system is of great importance for increase in solubility of hydrophobic drugs and therapy efficiency. The unique core-shell architecture of the copolymer micelles provides the possibility for the capture and delivery of hydrophobic drugs, where their hydrophobic cores can accommodate hydrophobic drugs and the hydrophilic shells supply the copolymer micelles even drugs the stability. HCPT is a cancer chemotherapy drug that is used to treat stomach cancer, liver cancer, and leukemia. However, HCPT's insolubility and hydrolysis of active lactone rings in physiological media or aqueous solutions have limited its applications. Considering these factors, HCPT was used as a model drug to be loaded in the hydrophobic core of the micelles by dialysis, and the EE is determined to be 31.4–32.5%. This value is higher than the value reported previously.[40]

The HCPT delivery from $C_3$-(PS-*b*-PNIPAM) copolymer micelles was examined by determining cumulative drug release with time at various temperatures in simulated physiological media, as presented in Figure 6. It is clear that the release of HPCT from the two drug formulations is thermo-triggered and compositional-dependent or dependent on the length ratios of hydrophilic/hydrophobic blocks. The cumulative release amount of HPCT from the two drug formulations is only 33.7% at a release time of 24 h at pH of 7.4 and temperature 25°C (<LCST), and 64.8 and 71.4% at a release time of 97 h. However, when the solution temperature is increased to 37°C (>LCST), the drug release amount reaches up to 47.8 and 54.2% after 24 h, and 85.0 and 94.5% at a release time of 97 h, corresponding to $C_3$-(PS-*b*-PNIPAM)$_2$ and $C_3$-(PS-*b*-PNIPAM)$_1$, respectively. This faster drug release rate and higher release amount above LCST than below LCST are ascribed to temperature-induced structural alterations of copolymer micelles.[41,42] Whereas the dependence of the drug release on copolymer compositions is presumably correlated with the length ratios of hydrophilic/hydrophobic blocks as well as the resultant hydrophilic/hydrophobic balance. Longer PNIPAM hydrophilic chains or molecular weights have better stabilization for the hydrophobic core of micelles, and hence the HCPT-loaded $C_3$-(PS-*b*-PNIPAM)$_2$ drug formulation leads to relatively slow HCPT release.

Conversely, it is noticed that no initial burst drug release appears in the copolymer micelle-based drug formulations, and the drug release of HCPT is gradually increased with time. Even above LCST, the copolymer micelle-based drug formulations still contain sufficient drug contents for effective therapy and can last for 4 days (97 h). This is related to the good capture in the hydrophobic inner cores of the copolymer micelles, not on the micelle surfaces, as expected, which makes HCPT sustainedly release by diffusion.
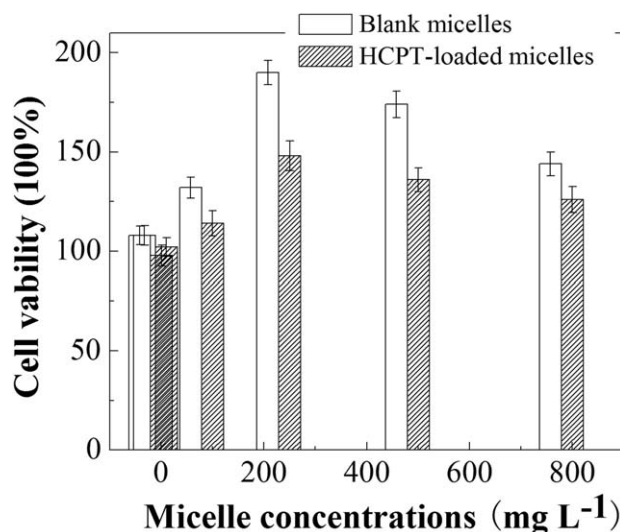


**Figure 7. Cell cytotoxicities of blank and HCPT-loaded (LC: 6.28%) $C_3$-(PS-*b*-PNIPAM) copolymer micelles (Micelle concentration: 1–800 mg L$^{-1}$) against L929 cell lines after 48 h incubation.**

Therefore, it can be inferred that the engineered copolymer micelles can keep reasonable drug encapsulation and release, and the release behavior can be tuned by changing environmental temperature and/or regulating proper copolymer composition or block degrees of polymerization.

### Cytotoxicity studies

Biocompatibility is vital for applications of polymer materials in drug delivery system. To evaluate the *in vitro* cytotoxicity of the copolymer micelles, the MTT assay was performed. Figure 7 shows the proliferation results of L929 cells treated with the blank and HCPT-loaded $C_3$-(PS-*b*-PNIPAM) copolymer micelles with concentrations from 1 to 800 mg $L^{-1}$ after 48 h incubation. It is clearly seen that there is no significant difference in cell viabilities for the blank and HCPT-loaded copolymer micelles in the examined micelle concentration range ($P < 0.05$). Although the HCPT-loaded copolymer micelles produce relatively decreased cell viabilities due to a little amount of the *in vitro* drug release, the values are above 98%, hinting that the copolymer micelles are nontoxic. Consequently, the HCPT encapsulation in the copolymer micelle may remarkably decrease drugs' harm to normal cells before they arrive at lesion sites. It is worth noting that the cell viabilities are above 100% for almost all copolymer micelles in Figure 7. This is probably due to the unique architecture of the three-arm star block copolymers, which is beneficial to the cell growth and proliferation. In fact, in the group of the cultured cells, there exist cell adhesion, cell growth, cell spreading, cell division, and proliferation besides cell death. The cell growth and proliferation result in the cell viability higher than 100%. It is anticipated that the nontoxic copolymer micelle-based drug formulations can potentially be used as a safe drug delivery carrier in biomedical applications.

## Conclusion

Well-defined starlike $C_3$-(PS-*b*-PNIPAM) block copolymers have successfully been prepared by combination of esterification reaction, aminolysis reaction, and successive ATRP. These star copolymers can spontaneously assemble into core-shell spherical micelle aggregates in aqueous solution, with CAC values from ca 11.62 to 47.61 mg $L^{-1}$, and hydrodynamic diameters of about 200–220 nm. The LCST values slightly vary with compositional ratios or molecular weights of the two blocks. The water-insoluble HCPT can effectively be entrapped into the hydrophobic cores of the micelles, and the *in vitro* drug release profiles exhibit temperature-induced sustained HCPT release. The resulting physicochemical parameters are not significantly influenced by the drug encapsulation. Therefore, the micelle aggregates can safely deliver HCPT at lesion sites without early destruction. The HCPT-loaded copolymer micelles are demonstrated to have no apparent cytotoxicity against the cultured cells, and thus avoid harm to normal cells before they arrive at lesion sites. Hence, the copolymer micelle systems are an effective and promising platform in the formulation design of poorly-soluble HCPT drug, and effective drug delivery and therapy can be achieved by changing the copolymer composition and environmental temperature.

## Acknowledgment

## Literature Cited

1. Hawker CJ, Hedrick JL. Accurate control of chain ends by a novel "living" free-radical polymerization process. *Macromolecules.* 1995; 28:2993–2995.
2. Hawker CJ, Grubbs RB, Dao J. Preparation of hyperbranched and star polymers by a "living", self-condensing free radical polymerization. *J Am Chem Soc.* 1995;117:10763–10764.
3. Chong YK, Le TPT, Moad G, Rizzardo E, Thang SH. A more versatile route to block copolymers and other polymers of complex architecture by living radical polymerization: the raft process. *Macromolecules.* 1999;32:2071–2074.
4. Kïrcï B, Lutz JF, Matyjaszewski K. Synthesis of well-defined alternating copolymers poly(methylmethacrylate-*alt*-styrene) by raft polymerization in the presence of Lewis acid. *Macromolecules.* 2002;35: 2448–2451.
5. Krzysztof M. Atom transfer radical polymerization (ATRP): current status and future perspectives. *Macromolecules.* 2012;45:4015–4039.
6. Cui GH, Li YH, Shi TT, Gao ZG. Synthesis and characterization of Eu(Ш) complexes of modified cellulose and poly(N-isopropylacrylamide). *Carbohydr Polym.* 2013;94:77–81.
7. Wang DQ, Tan JJ, Kang HL, Ma L. Synthesis, self-assembly and drug release behaviors of pH-responsive copolymers ethyl cellulose-graft-PDEAEMA through ATRP. *Carbohydr Polym.* 2011;84:195–202.
8. Kizhakkedathu JN, Kumar KR, Goodman D, Brooks DE. Synthesis and characterization of well-defined hydrophilic block copolymer brushes by aqueous ATRP. *Polymer.* 2004;45:7471–7489.
9. Zhao YL, Chen YM, Chen CF, Xi F. Synthesis of well-defined star polymers and star block copolymers from dendrimer initiators by atom transfer radical polymerization. *Polymer.* 2005;46:5808–5819.
10. Liu R, Li ZD, Yuan D, Meng CF, Wu Q, Zhu FM. Synthesis and self-assembly of miktoarm star copolymers of (polyethylene)₂-(poly-styrene)₂. *Polymer.* 2011;52:356–362.
11. Zhang WD, Zhang W, Zhou NC, Cheng ZP. Synthesis and self-assembly behaviors of three-armed amphiphilic block copolymers via RAFT polymerization. *Polymer.* 2008;49:4569–4575.
12. Stenzel-Rosenbaum MH, Davis TP, Fane AG, Chen V. Porous polymer films and honeycomb structures made by the self-organization of well-defined macromolecular structures created by living radical polymerization techniques. *Angew Chem Int Ed.* 2001;40:3428–3432.
13. Tao L, Catherine K, Rachel R. Synthesis of maleimide-end-functionalized star polymers and multimeric protein-polymer conjugates. *Macromolecules.* 2009;42:8028–8033.
14. Heise A, Hedrick JL, Frank CW, Miller RD. Starlike block copolymers with amphiphilic armsas models for unimolecular micelles. *J Am Chem Soc.* 1999;121:8647–8648.
15. Huh J, Kim KH, Ahn CH, Jo WH. Micellization behavior of star-block copolymers in a selective solvent: a brownian dynamics simulation approach. *J Chem Phys.* 2004;121:4998–5004.
16. Tao W, Zeng XW, Liu T, Wang ZY, Xiong QQ, Ouyang CP, Huang LQ, Mei L. Docetaxel-loaded nanoparticles based on star-shaped mannitol-core PLGA-TPGS diblock copolymer for breast cancer therapy. *Acta Biomater.* 2013;9:8910–8920.
17. Soliman GM, Sharma R, Choi AO, Varshney SK. Tailoring the efficacy of nimodipine drug delivery using nanocarriers based on $A_2B$ miktoarm star polymers. *Biomaterials.* 2010;31:8382–8392.
18. Rezaei SJT, Nabid MR, Niknejad H, Entezami AA. Multifunctional and thermoresponsive unimolecular micelles for tumor-targeted delivery and site-specifically release of anticancer drugs. *Polymer.* 2012;53:3485–3497.
19. Fay F, McLaughlin KM, Small DM. Conatumumab (AMG 655) coated nanoparticles for targeted pro-apoptotic drug delivery. *Biomaterials.* 2011;32:8645–8653.
20. Su ZG, Shi YP, Xiao YY. Effect of octreotide surface density on receptor-mediated endocytosis in vitroand anticancer efficacy of modified nanocarrier in vivo after optimization. *Int J Pharm.* 2013; 447:281–292.
21. Wei H, Zhang XZ, Cheng C, Cheng SX, Zhuo RX. Self-assembled, thermosensitive micelles of a star block copolymer based on PMMA and PNIPAAm for controlled drug delivery. *Biomaterials.* 2007;28: 99–107.
22. Rezaei SJT, Nabid MR, Niknejad H, Entezami AA. Folate-decorated thermoresponsive micelles based on star-shaped amphiphilic block copolymers for efficient intracellular release of anticancer drugs. *Int J Pharm.* 2012;437:70–79.
23. Hirao A, Inushima R, Nakayama T, Watanabe T, Yoo HS, Deffieux A. Precise synthesis of thermo-responsive and water-soluble star-

branched polymers and star block copolymers by living anionic polymerization. *Eur Polym J*. 2011;47:713–722.

24. Cui SX, Pang XC, Zhang S, Yu Y. Unexpected temperature-dependent single chain mechanics of poly(N-isopropyl-acrylamide) in Water. *Langmuir*. 2012;28:5151−5157.

25. Wang JS, Zhao HB, Ge XG, Liu Y, Chen L. Novel flame-retardant and antidripping branched polyesters prepared via phosphorus-containing ionic monomer as end-capping agent. *Ind Eng Chem Res*. 2010;49:4190–4196.

26. Jin L, Hang WW, Sun JJ, Wu HX, Yang SP. Synthesis and study on the complex formation with copper ions of dendritic polyamide-amine molecules. *J. Shanghai Normal Uni. (Natural Sci.)* 2007;36: 73–78.

27. Bera RK, Sharma D, Sahoo SK, Kanungo BK. Potentiometric study of a benzene-based tripodal triamine as chelator for Zn(II) Ion. *Acta Chim Slov*. 2011;58:590–595.

28. Wörl R, Köster H. Synthesis of new liquid phase carriers for use in large scale oligonucleotide synthesis in solution. *Tetrahedron*. 1999; 55:2941–2956.

29. Wörl R, Köster H. The use of liquid phase carriers for large scale oligonucleotide synthesis in solution via phosphoamidite chemistry. *Tetrahedron*. 1999;55:2957–2972.

30. Sawicki M, Lecercle D, Grillon G, Gall BL. Bisphosphonate sequestering agents. Synthesis and preliminary evaluation for in vitro and in vivo uranium(VI) chelation. *Eur J Med Chem*. 2008;43:2768–2777.

31. Matsuura K, Murasato K, Kimizuka N. Artificial peptide-nanospheres self-assembled from three-way Junctions of *β*-sheet-forming peptides. *J Am Chem Soc*. 2005;127:10148–10149.

32. Wang GJ, Wang XG. A novel hyperbranched polyester functionalized with azochromophore: synthesis and photoresponsive properties. *Polym Bull*. 2002;49:1–8.

33. Lu XJ, Zhang LF, Meng LZ, Liu YH. Synthesis of poly(N-isopropy-lacryl- amide) by ATRP using a fluorescein-based initiator. *Polym Bull*. 2007;59:195–206.

34. Furyk S, Zhang Y, Ortiz-Acosta D, Cremer PS, Bergbreiter DE. Effects of end group polarity and molecular weight on the lower critical solution temperature of poly(*N*-isopropylacrylamide). *J Polym Sci Part A: Polym Chem*. 2006;44:1492–1501.

35. Laukkanen A, Valtola L, Winnik FM, Tenhu H. Formation of colloidally stable phase separated poly(*N*-vinylcaprolactam) in water: a study by dynamic light scattering, microcalorimetry, and pressure perturbation calorimetry. *Macromolecules*. 2004;37:2268–2274.

36. Xia Y, Burke NAD, Stöver HDH. End group effect on the thermal response of narrow-disperse poly(*N*-isopropylacrylamide) prepared by atom transfer radical polymerization. *Macromolecules*. 2006;39: 2275–2283.

37. Deng C, Jiang YJ, Cheng R, Meng FH, Zhong ZY. Biodegradable polymeric micelles for targeted and controlled anticancer drug delivery: promises, progress and prospects. *Nano Today*. 2012;7:467–480.

38. Zhang L, Lin Y, Zhang Y, Chen R, Zhu Z, Wu W, Jiang X. Fluorescent micelles based on star amphiphilic copolymer with a porphyrin core for bioimaging and drug delivery. *Macromol Biosci*. 2012;12: 83–92.

39. Neha MD, Pranav BP, Anita PA, Vilasrau JK. Polymeric micelles as a drug carrier for tumor targeting. *Chron Young Sci* 2013;4:94–101.

40. Sun XT, Wang JL, Li LB. Mixed micelles made of pluronic P105 and L61 as pharmaceutical nanocarriers for camptothecin. *J Shandong Uni (Heath Sci)*. 2009;47:128–131.

41. Yang Z, Xie J, Zhou W, Shi W. Temperature sensitivity and drug encapsulation of star-shaped amphiphilic block copolymer based on dendritic poly(ether-amide). *J Biomed Mater Res A*. 2009;89:988–1000.

42. Feng Z, Lin L, Yan Z, Yu Y. Dual Responsive block copolymer micelles functionalized by NIPAM and azobenzene. *Macromol Rapid Commun*. 2010;31:640–644.